Photocatalytic Dimerization of Olefins by Decatungstate(VI), $[W_{10}O_{32}]^{4-}$, in Acetonitrile and Magnetic Resonance Studies of Photoreduced Species †

Toshihiro Yamase * and Takashi Usami
Research Laboratory of Resources Utilization, Tokyo Institute of Technology, 4259 Nagatsuta, Midori-ku, Yokohama 227, Japan

U.v. photolysis of homogeneous solutions containing tetrakis(tetrabutylammonium) decatungstate(VI), $[NBu_4]_4[W_{10}O_{32}]$, and olefins in acetonitrile leads to dimerization of olefins *via* abstraction of an allyl hydrogen, with accompanying formation of reduced decatungstates, up to two electrons. Coexistence of heterogeneous catalysts such as RuO_2 and Pt results in a hydrogen-forming reoxidation of the protonated reduced decatungstate to $[W_{10}O_{32}]^{4-}$, establishing a catalytic dimerization of olefins with evolution of hydrogen. The photoassisted catalytic dimerization is sustained over 50 h. Flash photolysis experiments indicate that the O ⟶ W charge-transfer excited state of $[W_{10}O_{32}]^{4-}$ undergoes an electron transfer from olefins to yield $[W_{10}O_{32}]^{5-}$. Production of $[W_{10}O_{32}]^{5-}$ is followed by protonation to give $[HW_{10}O_{32}]^{4-}$ (pK_a for $[HW_{10}O_{32}]^{4-}$ = 5.4 ± 0.5), which competes with a back reaction between $[W_{10}O_{32}]^{5-}$ and a semi-oxidized olefin with a rate constant of (7.2 ± 0.2) × 10^{10} dm^3 mol^{-1} s^{-1}. Disproportionation of $[HW_{10}O_{32}]^{4-}$ to $[H_2W_{10}O_{32}]^{4-}$ and $[W_{10}O_{32}]^{4-}$ occurs with rate constants of (2.6—10.3) × 10^4 dm^3 mol^{-1} s^{-1} which increase with increasing ratio of olefin concentration in the solvents. The peak to peak linewidth (ΔH_{pp} = 20 G) of the e.s.r. signal due to $[W_{10}O_{32}]^{5-}$ or $[HW_{10}O_{32}]^{4-}$ is almost constant over the range 4.4—100 K. In connection with the single-crystal e.s.r. spectrum of $[HW_{10}O_{32}]^{4-}$ at 77 K, this is attributed to the semi-occupied molecular orbital consisting of orbital mixing among four sets of O=W–O–W=O multiple bonds at eight equatorial WO_6 sites. At temperatures higher than 100 K, line broadening with increasing temperature is observed and gives an activation energy of 0.06 eV for an electron hopping between equatorial and capped WO_6 sites. ^{183}W N.m.r. chemical shifts for $[H_2W_{10}O_{32}]^{4-}$ are discussed in terms of two effects on the electron delocalization, the orbital-mixing delocalization among equatorial WO_6 sites and the thermally activated hopping process between equatorial and capped WO_6 sites (at T > 100 K): the former results in an upfield shift relative to the resonance for the eight equatorial W atoms of $[W_{10}O_{32}]^{4-}$, while the latter causes a downfield shift relative to the resonance for the two capped W atoms.

In the course of our investigation of photoredox reactions of polyoxometalates with water, alcohols, carboxylic acids, and alkynes,[1–6] we have paid special attention to an ability of the polyoxometalates to photo-oxidize various organic substances with high selectivity.[7,8] Recently, we found a photosensitized dimerization of olefins by tetrakis(tetrabutylammonium) decatungstate(VI) $[NBu_4]_4[W_{10}O_{32}]$ in acetonitrile (CH_3CN): the reaction does not occur in the absence of $[W_{10}O_{32}]^{4-}$ and the mechanism is not fully established yet.[9] The photochemistry of $[NBu_4]_4[W_{10}O_{32}]$ in CH_3CN indicates that photoexcitation of the O ⟶ W charge-transfer band for $[NBu_4]_4[W_{10}O_{32}]$ in CH_3CN induces an electron transfer from $[NBu_4]^+$ to $[W_{10}O_{32}]^{4-}$ yielding but-1-ene, $[NBu_3]^{\cdot+}$, a proton, and $[W_{10}O_{32}]^{5-}$. The species $[W_{10}O_{32}]^{5-}$ is protonated and converted to a protonated two-electron reduction species, $[H_2W_{10}O_{32}]^{4-}$, as a result of the disproportionation of $[HW_{10}O_{32}]^{4-}$.[3] This paper describes the mechanistic details for the photoredox reaction between $[NBu_4]_4[W_{10}O_{32}]$ and olefins (especially cyclohexene) and establishes a photocatalytic dimerization of olefins evolving dihydrogen gas in the presence of heterogeneous RuO_2 catalysts. Only a few photodimerizations of olefins by inorganic photosensitizers have been published: u.v. photolysis of η^3-allyl–palladium complexes in CH_3CN gives 1,5-dienes in good yields *via* homolytic cleavage of a carbon–palladium bond.[10] But, unfortunately, the reaction does not proceed catalytically, in contrast to the present work.

In this paper, furthermore, based on the fact that the structure of the $W_{10}O_{32}$ frame is retained upon photoreduction,[11] structure indications obtained through e.s.r. and ^{17}O and ^{183}W n.m.r. experiments for the photolyte are discussed in terms of the delocalization of the added electrons in the anion.

Experimental

The preparation of $[NBu_4]_4[W_{10}O_{32}]$ described previously[3,12] was modified as follows: $[NBu_4]Br$ (2.4 g) and $Na_2[WO_4]\cdot 2H_2O$ (5.0 g) were each dissolved in hot water (90 °C, 1000 cm^3) adjusted to pH 2 with HCl. The two solutions were mixed and kept at 90 °C for 1 h. After cooling, a pale yellow precipitate was filtered off, washed with hot water (90 °C, and dried in air. Recrystallization was performed in acetonitrile–acetone (1:1 v/v) (Found: C, 22.95; H, 4.50; N, 1.70; W, 55.45. Calc. for $[NBu_4]_4[W_{10}O_{32}]$: C, 23.15; H, 4.35; N, 1.70; W, 55.40%). The purity of the product was checked by the u.v. spectrum ($\lambda_{max.}$ = 323 nm, ε = 1.35 × 10^4 dm^3 mol^{-1} cm^{-1} in CH_3CN), polarography (dropping mercury electrode, CH_3CN, $E_{\frac{1}{2}}$ = −0.85 V *vs.* Ag–AgCl),[3] and ^{17}O and ^{183}W n.m.r. spectra. The compound $K_5[BW_{12}O_{40}]\cdot 15H_2O$ was prepared according to previous procedures.[4,13] The six-electron reduction species of $[BW_{12}O_{40}]^{5-}$ was prepared by u.v. photolysis (λ > 310 nm) of $[BW_{12}O_{40}]^{5-}$ in the presence of CH_3OH at pH 0.3 according to the previous procedure.[4] The brown six-electron reduction

† *Non-S.I. units employed:* Torr ≈ 133 Pa, eV ≈ 1.6 × 10^{-19} J, G = 10^{-4} T.

species $[H_xBW_{12}O_{40}]^{x-}$ (probably, $x = 6$)[11] was precipitated as the potassium salt when the deaerated photolyte, obtained through prolonged photolysis, was cooled to 278 K. All other reagents were at least analytical grade and used as supplied.

Removal of water from CH_3CN and olefins was carried out by stirring them on 5 Å molecular sieves and filtering. The oxide RuO_2 was heated at 250 °C for 12 h prior to use. The evacuation to 10^{-4} Torr of solutions for measurements of absorption, e.s.r., and n.m.r. spectra and flash photolyses was carried out by several freeze–pump–thaw cycles. A 500-W super-high-pressure mercury lamp in conjunction with filters was used as a light source for the steady-state photolysis at room temperature. Light intensities at 365 nm were measured using potassium ferrioxalate actinometry.[14] Sample solutions (5 cm^3) for long-term photolyses in Pyrex tubes were deaerated with solvent-saturated nitrogen or argon. The solution containing the required amount of RuO_2 powder was continuously stirred at room temperature during the photoirradiation.

Analysis of W^V in the photolyte was carried out at room temperature by titration of an aqueous solution of $Fe(NO_3)_3$ under an atmosphere of nitrogen, which resulted in the disappearance of the blue colour due to W^V. Gas chromatography (Hitachi 164) on a Carbosieve S column was employed for the analysis of hydrogen. Oxidation products were measured by gas chromatography (Hitachi 163, FID detector) on a PEG-20M or Chromosorb 101 (for benzaldehyde) column. Oxidation products, olefin dimers, were isolated by column chromatography on silica gel eluting with n-hexane and identified by comparing g.c.–m.s. (gas chromatographic–mass spectra, Hitachi M80 g.c.–m.s. spectrometer) with those of authentic samples.[15] 3,3′-Dicyclohexene g.c.–m.s. (20 eV); *m/e* 162 (M^+, 4%), 81 (100); ^1H n.m.r. δ($CDCl_3$): 5.6 (m, 4 H), 1.8 (m, 14 H). 3,3′-Dicycloheptene g.c.–m.s. (70 eV); *m/e* 190 (M^+, 0.7%), 95 (100), 67 (18), 41 (7); ^1H n.m.r. δ($CDCl_3$): 5.6 (m, 4 H), 1.8 (m, 18 H). Dibenzyl g.c.–m.s. (70 eV); *m/e* 182 (M^+, 20%), 91 (100), 65 (15); ^1H n.m.r. δ($CDCl_3$), 7.0 (s, 10 H), 2.9 (s, 4 H). Citral ^1H n.m.r. δ ($CDCl_3$): 9.9 (d, 1 H), 9.8 (d, 1 H), 6.8 (d, 1 H), 5.1 (m, 1 H), 2.0—2.8 (m, 7 H), 1.7 (s, 3 H), 1.6 (s, 3H). Neral [(*Z*)-citral] g.c.–m.s. (70 eV); *m/e* 152 (M^+, 1.2%), 69 (64), 41 (100), 27 (23%). Geranial [(*E*)-citral] g.c.–m.s. (70 eV), *m/e* 152 (M^+, 5%), 69 (95), 41 (100).

Electronic spectra were recorded on a Hitachi 330 spectrophotometer. Flash-photolysis experiments on the hundreds of μs time-scale were carried out by using a conventional xenon-flash apparatus described previously.[3,4] Microsecond flash-photolysis experiments employed a 337-nm nitrogen laser (NRG 0.9–5–90), delivering a half-width of *ca.* 20 ns at 0.2 mJ per pulse. Transient absorptions of samples, placed in a 1-cm quartz fluorescence cell, were monitored using a xenon flash lamp (total lifetime *ca.* 100 μs) and the analyzing beam, passed through the cell 10° to the laser beam, was focused into the entrance slit of a 25-cm Nikon G-25 monochromator. In order to achieve high intensities, we concentrated the laser beam to an area of *ca.* 1 × 3 mm. This small area required that the analytical light must be carefully aligned in order to achieve a good overlap with the laser exciting beam. The light absorption was detected by a R636 Hamamatsu PM tube, connected to a Sony-Tektronix 475 oscilloscope. A transmitting glass filter (Toshiba VO-52, cut-off $\lambda < 520$ nm) was inserted between the slit of the monochromator and the sample cell. Nanosecond laser-flash photolysis was carried out by using a XeCl (308 nm) excimer laser, delivering a half-width of 10—14 ns at 10 mJ per pulse.

X-Band e.s.r. spectra were recorded on a Varian E12 spectrometer equipped with an Oxford Instruments cryostat (ESR 900) in order to perform experiments down to 4.4 K. Oxygen-17 and ^{183}W n.m.r. spectra were obtained in a thermostatted 10-mm diameter n.m.r. tube (at 300 K) using JEOL GX270 and GX500 spectrometers, respectively. The ^{17}O and ^{183}W chemical shifts were referenced to external water and 2 mol dm^{-3} $Na_2[WO_4]$, respectively. Approximately 1 g of $[NBu_4]_4[W_{10}O_{32}]$ was contained in CD_3CN (2.3 cm^3) and cyclohexene (0.7 cm^3). The sample was then irradiated for 3 d with light, $\lambda > 310$ nm, allowing the paramagnetic one-electron reduced decatungstate to be converted to a diamagnetic two-electron reduced decatungstate.[3] The spectra of dodecatungstoborates were obtained on thermostatted 10-mm diameter D_2O solutions at 300 K.

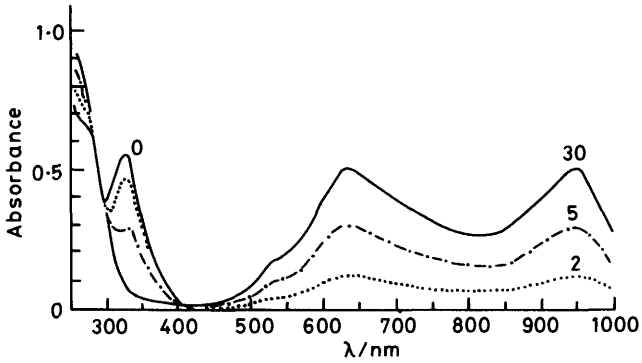

Figure 1. Spectral changes upon 365-nm light (1.47×10^{-4} einstein dm^{-3} min^{-1}) irradiation of a deaerated solution containing 4.1×10^{-5} mol dm^{-3} $[NBu_4]_4[W_{10}O_{32}]$ and 0.5 mol dm^{-3} cyclohexene in CH_3CN. Times (min) are indicated on the curves. Optical pathlength: 10 mm

Table 1. Long-term photolysis of deaerated solutions containing 0.5 mol dm^{-3} cyclohexene and various concentrations of $[NBu_4]_4[W_{10}O_{32}]$ in CH_3CN *

$[NBu_4]_4[W_{10}O_{32}]$ concentration/ mmol dm^{-3}	Irradiation time/h	W^V/mmol dm^{-3}	3,3′-Dicyclohexene/ mmol dm^{-3}
5	2	11.0	4.3
7.5	3	14.0	6.5
10	3.5	18.4	8.1
12.5	4.5	23.0	10.5
15	5	28.0	13.0

* Photolysis was done under $\lambda > 310$ nm light irradiation.

Results

Steady-state Photolysis.—An absorption maximum at 323 nm in CH_3CN is characteristic of $[W_{10}O_{32}]^{4-}$, due to O ⟶ W charge-transfer absorption at the nearly linear W–O–W bond.[11,16] The absorption band at $\lambda_{max.} = 323$ nm is hardly changed in the presence of cyclohexene. Photolysis ($\lambda = 365$ nm) of solutions containing 4.1×10^{-5} mol dm^{-3} $[NBu_4]_4[W_{10}O_{32}]$ and 0.5 mol dm^{-3} cyclohexene in CH_3CN results in a decrease of the 323-nm absorption peak with simultaneous development of absorption bands at 630 and 945 nm associated with intervalence charge-transfer bands for protonated reduced decatungstates.[3,11] The photosensitized oxidation of cyclohexene by $[W_{10}O_{32}]^{4-}$ leads to formation of 3,3′-dicyclohexene as the main oxidation product. Figure 1 shows a change in the absorption spectrum of the solution during the photolysis. As shown in Table 1, the results for long-term photolysis of solutions containing $[NBu_4]_4[W_{10}O_{32}]$ and cyclohexene indicate that the amount of 3,3′-dicyclohexene (two-electron oxidized product of cyclohexene) is nearly equal to the initial concentration of $[NBu_4]_4[W_{10}O_{32}]$ and that there is an approximate

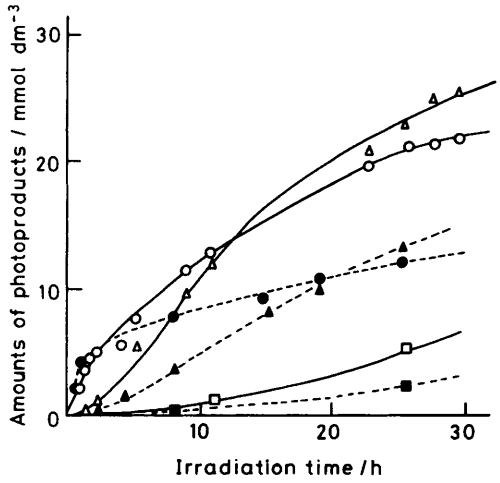

Figure 2. Plot of amounts of products against irradiation time ($\lambda > 313$ nm) for deaerated solutions (5 cm^3) containing 5.0 mmol dm^{-3} $[NBu_4]_4[W_{10}O_{32}]$, 0.5 mol dm^{-3} cyclohexene, and 5 mg (– – –) or 40 mg (——) RuO_2 in CH_3CN: 3,3′-dicyclohexene (○, ●), H_2 (△, ▲), cyclohexene trimers (□, ■)

relationship of 2:1 between W^V and 3,3′-dicyclohexene concentrations. Displacement from the stoicheiometric relationship is ascribed to formation of the trimer of cyclohexene as the other oxidation product, as described below. Table 1 suggests that $[W_{10}O_{32}]^{4-}$ is photochemically reduced, by up to two electrons. The quantum yield of 3,3′-dicyclohexene increases with increasing concentration of cyclohexene and approaches a plateau (= 0.06) at the cyclohexene concentration of 0.7 mol dm^{-3}.

Removal of $[NBu_4]_4[W_{10}O_{32}]$ from the solution results in no observable formation of 3,3′-dicyclohexene. The rate of formation of 3,3′-dicyclohexene, estimated from nearly linear portions of plots of 3,3′-dicyclohexene concentration against irradiation time, was linearly dependent upon the light intensity. The photoreduced decatungstates were reoxidized to $[W_{10}O_{32}]^{4-}$ in the presence of heterogeneous catalysts of RuO_2 and Pt with accompanying formation of H_2, as expected from the previous results for the photochemistry of $[NBu_4]_4[W_{10}O_{32}]$ in CH_3CN.[3] The necessity for heterogeneous catalysts for the reoxidation may be associated with the protonated reduced decatungstate, which is adsorbed strongly on the oxide surface.[4] Figure 2 shows the photocatalytic H_2 formation for the solutions containing 5.0 mmol dm^{-3} $[NBu_4]_4[W_{10}O_{32}]$, 0.5 mol dm^{-3} cyclohexene, and different amounts of RuO_2. An approximately stoicheiometric relationship between amounts of W^V, H_2, 3,3′-dicyclohexene, and cyclohexene trimer was maintained at each stage of the photolysis. Prolonged u.v. irradiation in the presence of RuO_2 results in a large amount of H_2 compared with 3,3′-dicyclohexene, due to cyclohexene trimer formation. Large amounts of RuO_2 increase the rate of H_2 formation, leading to a turnover number of more than 10 for 8 mg cm^{-3} RuO_2.

Similarly, photocatalytic dimerization of other olefins in the presence of RuO_2 was observed as summarized in Table 2. Geraniol, cyclohex-2-en-1-ol, and benzyl alcohol were converted exclusively to the corresponding carbonyl compounds, indicating that the alcoholic OH function interferes with dimerization of the allyl group. Quantum yields for dicyclopentene and dicyclohexene were higher than those of dicycloheptene and dicyclo-octene. Furthermore, stereochemically hindered olefins such as norbornadiene (bicyclo[2.2.1]hepta-2,5-diene) and camphene gave no observable dimer formation. These results suggest that the dimerization of

Table 2. Products of the photoreaction of $[W_{10}O_{32}]^{4-}$ with olefins in the presence of RuO_2[a]

Olefin	Product detected	Isomers	Relative quantum yield
	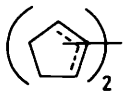	Two isomers[b] Trimers of two isomers[b]	0.9
	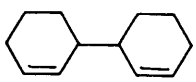	Trimers of four isomers[b]	1.0
	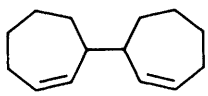		0.6
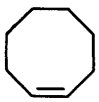	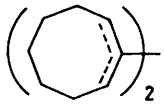	Two isomers[b]	0.3
	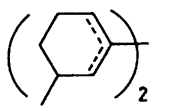	Two isomers[b]	0.3
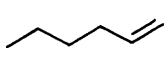	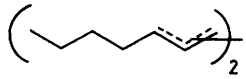	Two isomers[b]	0.4
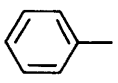	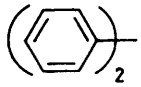		0.1
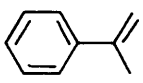	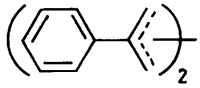	Two isomers[b]	0.2
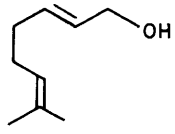	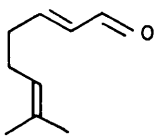	*c*	2.0
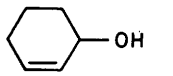	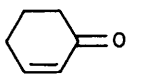	*d*	2.6
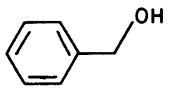	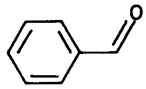	*d*	5.0
	No reaction		
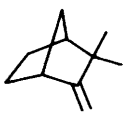	No reaction		

[a] Deaerated solution (5 cm^3) containing 10 mmol dm^{-3} $[NBu_4]_4[W_{10}O_{32}]$, 0.5 mol dm^{-3} olefin, and 20 mg RuO_2 in CH_3CN was photolyzed for 3 h under 310-nm light irradiation. [b] Each of the isomers was not identified. [c] Geranial was a photo-oxidation product but underwent photoisomerization to neral during prolonged photolysis. At 95% consumption of geraniol, the ratio of geranial to neral was 4:1. Removal of $[W_{10}O_{32}]^{4-}$ resulted in no photo-oxidation of geraniol. [d] No dimerization of a substrate occurred.

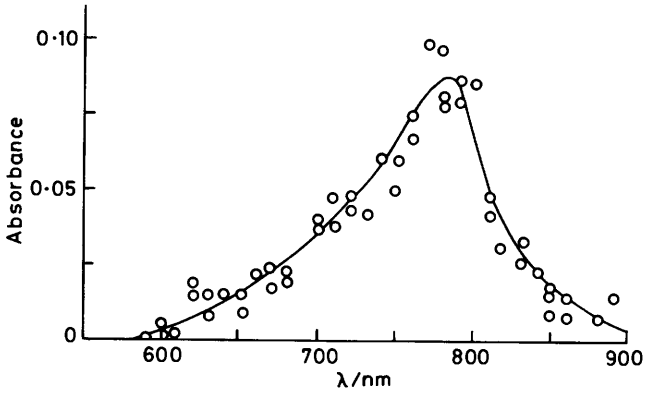

Figure 3. Transient spectrum obtained 2 μs after 337-nm laser pulse exposure of a deaerated solution containing 1.0 mmol dm^{-3} $[NBu_4]_4[W_{10}O_{32}]$ and 0.5 mol dm^{-3} cyclohexene in CH_3CN at room temperature. Optical pathlength of the cell is 10 mm

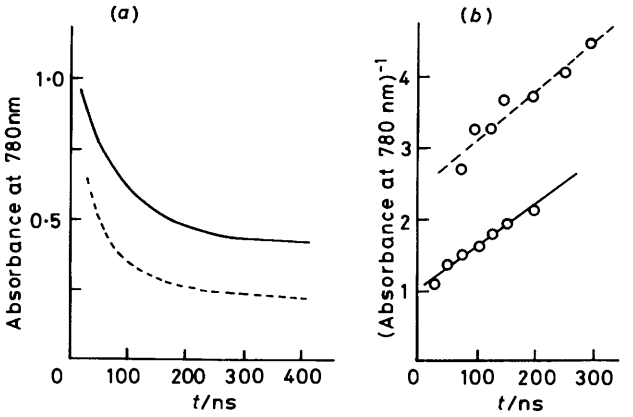

Figure 4. Decays (*a*) of transients produced in the 308-nm laser flash photolysis of 0.3 mmol dm^{-3} $[NBu_4]_4[W_{10}O_{32}]$ in the absence (----) and in the presence of 0.5 mol dm^{-3} cyclohexene (——). Lines (*b*) represent (absorbance at 780 nm)$^{-1}$ *vs.* *t* second-order kinetics plots. Optical pathlength of the cell is 10 mm

olefins results from u.v.-induced formation of a charge-transfer complex between the $W_{10}O_{32}$ frame and olefin.[4]

Laser-flash Photolysis.—Figure 3 shows a transient absorption spectrum, obtained 2 μs after the 337-nm laser pulse exposure of a deaerated solution containing 1.0 mmol dm^{-3} $[NBu_4]_4[W_{10}O_{32}]$ and 0.5 mol dm^{-3} cyclohexene in CH_3CN. The transient spectrum showing $\lambda_{max.} \approx 780$ nm (Figure 3) was obtained irrespective of the presence of cyclohexene. A similar spectrum was obtained 0.5 ms after a 100-μs flash photolysis.[3] Thus, the blue species produced by the laser pulse can be assigned to the unprotonated one-electron reduced species, $[W_{10}O_{32}]^{5-}$ [equation (1)], as discussed previously.[3] Assuming an absorption coefficient of $\varepsilon_{780} = 1.1 \times 10^4$ dm^3 mol^{-1} cm^{-1} [3] under the present experimental conditions, a single N_2-laser pulse converts *ca.* 0.84% of the ground-state population of $[W_{10}O_{32}]^{4-}$ into $[W_{10}O_{32}]^{5-}$. About 18.2% of the $[W_{10}O_{32}]^{4-}$ population for the deaerated solution containing 0.3 mmol dm^{-3} $[NBu_4]_4[W_{10}O_{32}]$ and 0.5 mol dm^{-3} cyclohexene in CH_3CN has been converted to $[W_{10}O_{32}]^{5-}$ by a single XeCl excimer-laser pulse (308 nm). Therefore, transient behaviour of $[W_{10}O_{32}]^{5-}$ was measured by the XeCl (308 nm) laser-pulse photolysis, since a high rate of $[W_{10}O_{32}]^{5-}$ formation in the 308-nm laser-flash photolysis made data analysis easier. Figure 4(*a*) shows oscillograms for $[W_{10}O_{32}]^{5-}$ obtained in the 308-nm laser-flash photolysis. The absorption of $[W_{10}O_{32}]^{5-}$ decays rapidly with a half-life of *ca.* 100 ns. As shown in Figure 4(*b*) the decay follows second-order kinetics and is attributed to the back reaction (2),[3] where $k_1 = (7.2 \pm 0.2) \times 10^{10}$ dm^3 mol^{-1} s^{-1} is almost unchanged irrespective of the presence of cyclohexene.

$$[W_{10}O_{32}]^{4-} + \text{C}_6\text{H}_{10} \xrightarrow{h\nu} [W_{10}O_{32}]^{5-} + \text{C}_6\text{H}_{10}^{\cdot+} + H^+ \quad (1)$$

$$[W_{10}O_{32}]^{5-} + \text{C}_6\text{H}_{10}^{\cdot+} + H^+ \xrightarrow{k_1} [W_{10}O_{32}]^{4-} + \text{C}_6\text{H}_{10} \quad (2)$$

Subsequent slow decay occurred and was investigated by 100-μs flash photolysis. The slow decay obeyed second-order kinetics involving disproportionation of the protonated one-electron reduced species $[HW_{10}O_{32}]^{4-}$, to $[H_2W_{10}O_{32}]^{4-}$ and $[W_{10}O_{32}]^{4-}$, as expected from the results for $[NBu_4]_4[W_{10}O_{32}]$ photolysis.[3] Reactions (3) and (4) denote the protonation and disproportionation processes, respectively. For

$$[W_{10}O_{32}]^{5-} + H^+ \rightleftharpoons [HW_{10}O_{32}]^{4-} \quad (3)$$

$$2[HW_{10}O_{32}]^{4-} \xrightarrow{k_2} [H_2W_{10}O_{32}]^{4-} + [W_{10}O_{32}]^{4-} \quad (4)$$

the disproportionation process, equations (5) and (6) can be derived, where K is the formation constant of $[HW_{10}O_{32}]^{4-}$, k_2 the rate constant for the disproportionation of $[HW_{10}O_{32}]^{4-}$, $[W_{10}{}^{5-}]_0$ the initial concentration of $[W_{10}O_{32}]^{5-}$, and $[H_2W_{10}{}^{4-}]_\infty$ the final concentration of $[H_2W_{10}O_{32}]^{4-}$.

$$1/[W_{10}{}^{5-}]^2 - 1/[W_{10}{}^{5-}]_0^2 = k_2Kt \quad (5)$$

$$1/([H_2W_{10}{}^{4-}]_\infty - [H_2W_{10}{}^{4-}]) - 1/([H_2W_{10}{}^{4-}]_\infty - [H_2W_{10}{}^{4-}]_0) = 2k_2t \quad (6)$$

Kinetic plots of A^{-2} against time (t), where A is the absorbance at 780 nm, are linear to 90% completion. The slope of such plots gives k_2K [equation (5)]. The secondary growth of the absorption (B) due to $[H_2W_{10}O_{32}]^{4-}$ was investigated at 630 nm as a function of the cyclohexene concentration, using $\varepsilon_{630} = 1.8 \times 10^4$ dm^3 mol^{-1} cm^{-1} for $[H_2W_{10}O_{32}]^{4-}$.[3] From plots of $(B_\infty - B)^{-1}$ against t, we can determine k_2 [equation (6)] and subsequently K, from the k_2K value. Figure 5(*a*) and (*b*) show kinetic plots of absorbances at 780 and 630 nm respectively, for the 100-μs flash photolysis of deaerated solutions of 1.0 mmol dm^{-3} $[NBu_4]_4[W_{10}O_{32}]$ with and without 0.5 mol dm^{-3} cyclohexene in CH_3CN. When the solution is aerobic (under an oxygen concentration of 3.0×10^{-4} mol dm^{-3}), $[W_{10}O_{32}]^{5-}$ decays with a rate constant of $k_3 = (3.8 \pm 0.8) \times 10^5$ dm^3 mol^{-1} s^{-1} to $[W_{10}O_{32}]^{4-}$ according to equation (7).

$$[W_{10}O_{32}]^{5-} + O_2 \xrightarrow{k_3} [W_{10}O_{32}]^{4-} + O_2^- \quad (7)$$

The data for a variety of cyclohexene concentrations are collected in Table 3. Table 3 indicates that k_2 is prone to

Table 3. Rate constants of the secondary spectral changes in the flash photolyses of deaerated $[W_{10}O_{32}]^{4-}$–cyclohexene CH_3CN solutions*

Cyclohexene concentration/ mol dm^{-3}	$10^{-10}k_1$/ dm^3 mol^{-1} s^{-1}	$10^{-4}k_2$/ dm^3 mol^{-1} s^{-1}	$10^{-5}k_3$/ dm^3 mol^{-1} s^{-1}	$10^{-5}K$/ dm^3 mol^{-1}	$pK_a = -\log K$ of $[HW_{10}O_{32}]^{4-}$	$10^{-3}\varepsilon_{630}$ of $[HW_{10}O_{32}]^{4-}$
0	7.0	2.6	4.5	7.2	5.9	
0.05		2.8		1.5	5.2	4.6
0.125		7.4		6.0	5.8	4.0
0.50	7.4	10.3	3.0	0.86	4.9	4.5
Average value	7.2 ± 0.2		3.8 ± 0.8		5.4 ± 0.5	4.4 ± 0.4

* Estimated values of k_2 (= 6 × 10^5 dm^3 mol^{-1} s^{-1}) and ε_{630} (≈ 2 × 10^3 dm^3 mol^{-1} cm^{-1}) for $[HW_{10}O_{32}]^{4-}$ in a previous paper[3] should be corrected to present values 2.6 × 10^4 dm^{-3} mol^{-1} s^{-1} and (4.4 ± 4) × 10^3 dm^3 mol^{-1} cm^{-1}, respectively.

Table 4. ^{17}O and ^{183}W n.m.r. chemical shifts (δ) of oxidized and two-electron reduced decatungstates*

	Terminal O	Bridging O: O_h environment	Bridging O: Approx. linear W–O–W	Bridging O: Others	Capped W	Equatorial W
Numbers of atom	10	2	4	16	2	8
$[W_{10}O_{32}]^{4-}$ at 300 K δ/p.p.m.	765.3	−6.5	420.4, 434.7		−160.2	−16.7
$[H_2W_{10}O_{32}]^{4-}$ at 300 K δ/p.p.m.	749.1	4.5	379.6	441.0	−82.9	−88.0
Change in δ upon reduction	−16.2	+11.0	−40.8 or −55.1	+20.6 or +6.3	+77.3	−71.3

* ^{17}O and ^{183}W n.m.r. chemical shifts are indicated relative to water and $Na_2[WO_4]$, respectively.

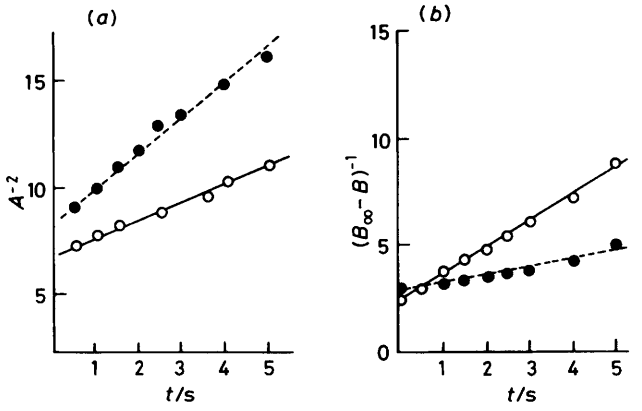

Figure 5. Plots of (*a*) A^{-2} *vs.* *t* and (*b*) $(B_\infty - B)^{-1}$ *vs.* *t* for the changes of transients *A* (780 nm) and *B* (630 nm) with (—○—) and without (--●--) 0.5 mol dm^{-3} cyclohexene. Optical pathlength of the cell is 96 mm

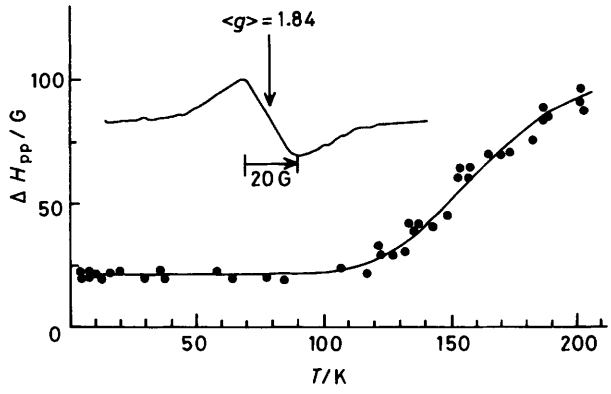

Figure 6. Temperature dependence of the e.s.r. linewidth (ΔH_{pp}) and e.s.r. signal at 4.4 K for the photolyte at a stage of photoreduction of 1.5 electrons added to $[W_{10}O_{32}]^{4-}$

increase slightly when decreasing the solvent polarity from a dielectric constant of ε 37.5 to 36.5 ($\varepsilon = \sum_i \varepsilon_i V_i$, where V_i is the volume fraction of component *i*). Amounts of $[W_{10}O_{32}]^{5-}$ and $[H_2W_{10}O_{32}]^{4-}$ produced by the flash pulse were proportional to the pulse intensity.

E.S.R. and ^{17}O *and* ^{183}W *N.M.R. Spectra.*—The photolyte exhibits a singlet-like e.s.r. signal of g = 1.84 with a peak to peak linewidth (ΔH_{pp}) of 20 G at 77 K, which is the same as for the photolysis of $[NBu_4]_4[W_{10}O_{32}]$ in CH_3CN.[3] The linewidth ΔH_{pp} is kept almost constant in the range 4.4—100 K but increases with increasing temperature (T) at T > 100 K. Figure 6 shows a plot of ΔH_{pp} against T, together with the e.s.r. signal of the photolyte, at 4.4 K, at the stage of 1.5-electron photoreduction of $[W_{10}O_{32}]^{4-}$. It is clear that, at T < 100 K where ΔH_{pp} is temperature independent, the paramagnetic electron delocalization is not due to the electron hopping which is thermally activated through vibrations of the decatungstate lattice.

Figures 7 and 8 show the ^{17}O (36.4 MHz frequency) and ^{183}W n.m.r. spectra (20.8 MHz), respectively. The ^{17}O and ^{183}W chemical shifts for $[W_{10}O_{32}]^{4-}$ were in good agreement with the location and intensity of the lines reported previously.[12,17] In the $[W_{10}O_{32}]^{4-}$ structure there are six types of non-equivalent oxygen atoms: the terminal oxygens appear as one line at 765.3 p.p.m. (relative intensity 5), while the doublet lines at 434.7 and 420.4 p.p.m. (intensity ratio 3:2) are due to the bridging oxygens. These assignments are based on the correlation between downfield chemical shift and oxygen π-bond order for the diamagnetic polyoxoanions.[12] Thus, the four bridging oxygens which bind the two halves of the anion with nearly linear W–O–W angles (170–179°)[11] may be assigned to a stronger line of the doublet, due to a significant amount of *dπ–pπ–dπ*, W–O–W bonding. The oxygens in octahedral environments appear as one line at −6.5 p.p.m. (relative

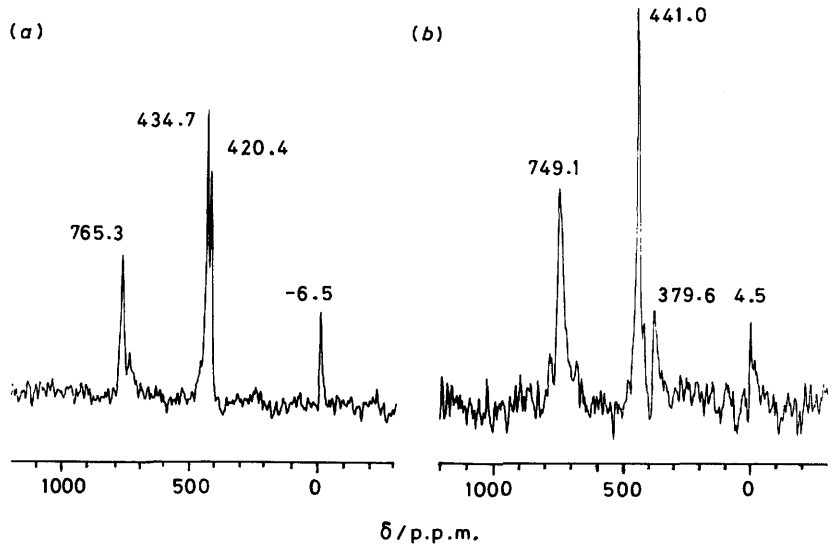

Figure 7. ^{17}O N.m.r. spectra (36.4 MHz) of $[NBu_4]_4[W_{10}O_{32}]$ in CD_3CN–cyclohexene before (*a*) and after (*b*) long-term photolysis

intensity 1). The ^{183}W n.m.r. spectrum shows two lines at −16.7 and −160.2 p.p.m. with a 4:1 intensity ratio, which correspond to two types of tungstens, equatorial and capped, in the $[W_{10}O_{32}]^{4-}$ structure. The ^{17}O n.m.r. spectrum of the photolyte [Figure 7(*b*)], containing approximately 100% $[H_2W_{10}O_{32}]^{4-}$, shows four lines at 749.1, 441.0, 379.6, and 4.5 p.p.m. with intensity ratio 5:8:2:1. The line (relative intensity 2) of chemical shift 379.6 p.p.m. indicates the four W–O–W oxygens that bind the two halves of the anion. The four lines of the 5:8:2:1 intensity ratio are shifted up-field, down-field, up-field, and down-field, respectively relative to the resonances for $[W_{10}O_{32}]^{4-}$. The ^{183}W n.m.r. spectrum of the photolyte [Figure 8(*b*)] shows two lines at −82.9 and −88.0 p.p.m. with a 1:4 intensity ratio, indicating that the line for the two capped tungstens is shifted down-field relative to the resonance for $[W_{10}O_{32}]^{4-}$, while that for the eight equatorial tungstens is shifted up-field. The assignment of resonances and chemical shifts for $[W_{10}O_{32}]^{4-}$ and $[H_2W_{10}O_{32}]^{4-}$ is summarized in Table 4.

Discussion

In studies of the photosensitized dimerization of olefins using organic photosensitizers such as 1-cyanonaphthalene and 9-cyanophenanthrene in CH_3CN, it has been proposed that the olefin dimer is formed *via* coupling of two allyl radicals which result from deprotonation of an olefin cation radical as shown in equation (8).[15,18–20]

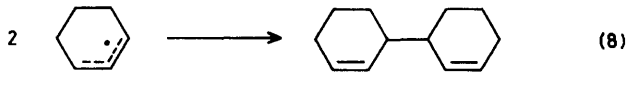

(8)

If the formation of 3,3′-dicyclohexene, based on this proposal, is treated by a steady-state method, the initial rate (R_d) of formation of 3,3′-dicyclohexene is given by $R_d = \varphi I/2$ where φ is the quantum yield of the allyl radical and I the intensity of the absorbed light. The linear relationship between R_d and the light intensity was observed, in good agreement with $R_d = \varphi I/2$. Furthermore, the fact that transient absorptions at 780 and 630 nm, produced by a single flash pulse, were linearly proportional to the pulse intensity, supports the occurrence of reactions (1)–(4), since each absorption can be assigned to $[W_{10}O_{32}]^{5-}$

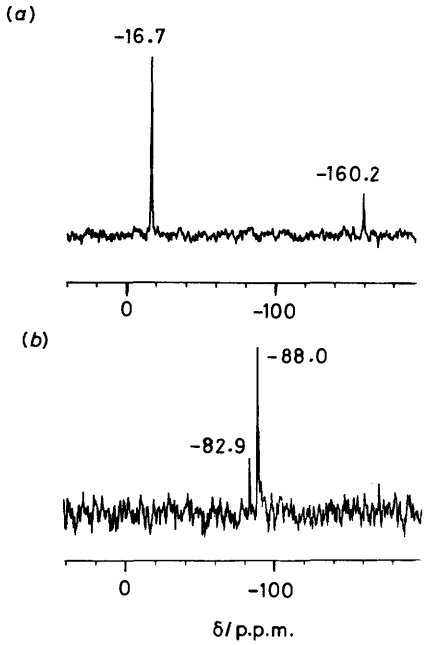

Figure 8. ^{183}W N.m.r. spectra (20.8 MHz) of $[NBu_4]_4[W_{10}O_{32}]$ in CD_3CN–cyclohexene before (*a*) and after (*b*) long-term photolysis

($\lambda_{max.}$ = 780 nm) and $[H_2W_{10}O_{32}]^{4-}$ ($\lambda_{max.}$ = 630 nm).[3] The possibility of reaction of the allyl radical with $[W_{10}O_{32}]^{4-}$ in the dark, yielding a carbonium cation and $[W_{10}O_{32}]^{5-}$, is unlikely, since the absorbance at 780 nm due to $[W_{10}O_{32}]^{5-}$ was not increased after the decay due to the recombination reaction of equation (2). In addition, the observable disproportionation of $[HW_{10}O_{32}]^{4-}$ to $[H_2W_{10}O_{32}]^{4-}$ and $[W_{10}O_{32}]^{4-}$ clearly excludes the possibility of a two-electron photoredox reaction between $[W_{10}O_{32}]^{4-}$ and cyclohexene.

E.s.r. spectra of the single crystal of diaquahydrogen tetrakis(di-isopropylammonium) decatungstate hexahydrate $[H(H_2O)_2][NH_2Pr^i_2]_4[W_{10}O_{32}]\cdot 6H_2O$ at 77 K, showing the superhyperfine interaction due to eight magnetically equivalent ^1H atoms at eight equatorial WO_6 sites, indicate the

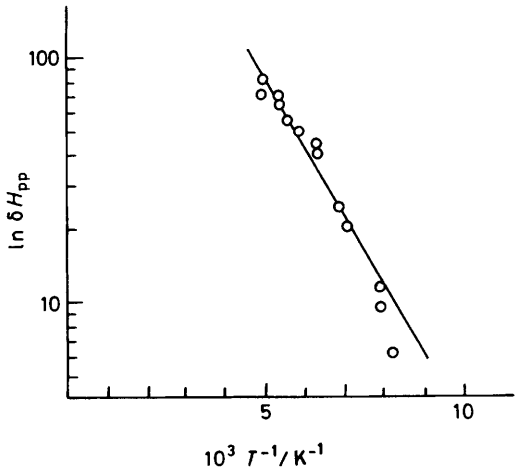

Figure 9. ln δH_{pp} as a function of temperature. δH_{pp} is the temperature-dependent part of the linewidth

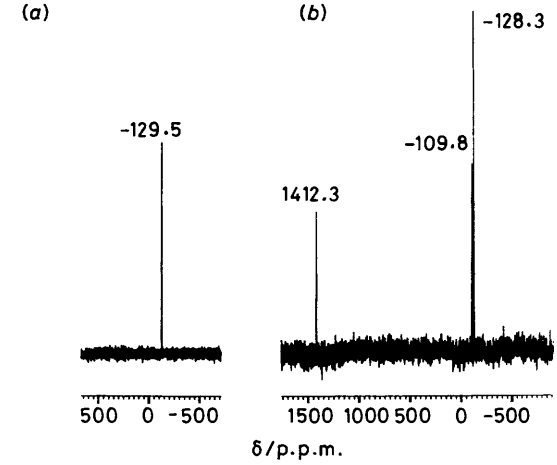

Figure 11. ^{183}W N.m.r. spectra (20.8 MHz) of 0.1 mol dm^{-3} $[BW_{12}O_{40}]^{5-}$ (*a*) and approximately 50 mmol cm^{-3} $[H_xBW_{12}O_{40}]^{x-11}$ (*b*) solutions

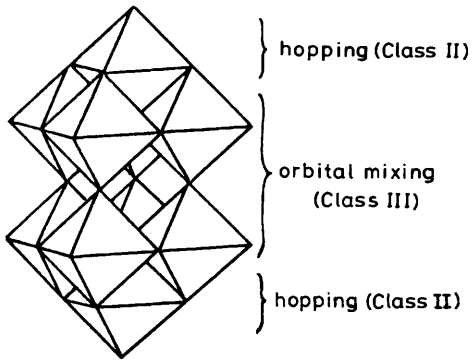

Figure 10. Two effects on the delocalization of the added electron in the decatungstate anion

delocalization of the paramagnetic electron among these sites.[11] Analysis of the e.s.r. parameters reveals that the semi-occupied molecular orbital (s.o.m.o.) forms orbital mixing among four orbital sets of the equatorial O=W–O–W=O multiple bonds which arrange two terminal W=O groups *cis* to the nearly linear W–O–W bridge moiety linking the two halves of the anion.[11] The constancy (ΔH_{pp} = 20 G) of the e.s.r. linewidth at $T \leqslant 100$ K (Figure 6) is explained by this s.o.m.o., since electron transfer in the s.o.m.o. does not require any thermal activation energy (E_{th}). Then, it is possible to say that, at $T < 100$ K, paramagnetic species of $[W_{10}O_{32}]^{5-}$ and $[HW_{10}O_{32}]^{4-}$ belong to Class III mixed-valence compounds.[21]

At high temperatures, $T > 100$ K, where ΔH_{pp} increases with temperature (Figure 6), thermally activated hopping is an added contribution to the paramagnetic electron delocalization. The activation energy, E_{th}, which would be required for electron hopping between the equatorial and capped WO_6 sites, can be deduced from an analysis of the ΔH_{pp} dependence with temperature (T), since e.s.r. linewidth broadening will arise from spin–lattice relaxation induced by the electron hopping.[4,22] Figure 9 represents a linear plot of ln $\delta H_{pp}(T)$ *vs.* T^{-1} [$\delta H_{pp} = \Delta H_{pp} - \delta H_{pp}(0)$, where $\delta H_{pp}(0)$ is the linewidth at 0 K], at $T > 120$ K. Assuming that $\delta H_{pp}(T)$ is proportional to the hopping frequency, $\nu = \nu_0 \exp(-E_{th}/kT)$,[23] we obtain E_{th} = 0.06 eV. The value is consistent with that for the electrochemically reduced species in dimethylformamide (dmf).[24] It is interesting to note that E_{th} = 0.06 eV is almost equal to the value (0.055 eV) for $[W_6O_{19}]^{3-}$,[25] for which the structure is six edge-shared octahedra corresponding to a half moiety of the $[W_{10}O_{32}]^{5-}$ lattice. Thus, the delocalization of the added electron in photoreduced decatungstates is described as a combination of two effects; the orbital-mixing delocalization (corresponding to Class III type) among the eight equatorial WO_6 sites and the thermally activated hopping process (corresponding to Class II type[21]) between the equatorial and capped WO_6 sites at high temperatures, $T > 100$ K. Figure 10 summarizes the two types of electron delocalization in the photoreduced decatungstate lattice. The mixture of delocalized and hopping valences has been suggested by e.s.r. results of the electrochemically reduced species in dmf but without any detailed characterization of the sites.[24] The coexistence of the two types of added electron delocalization in the anion at $T > 100$ K reveals establishment of a metal–semiconductor junction (Schottky junction) at the molecular level, since Class II and III mixed-valence compounds would correspond to semiconductor and metal, respectively.[21]

The two resonances with a 1:4 intensity ratio on the ^{183}W n.m.r. spectrum [Figure 8(*b*)] of the photolyte containing approximately 100% $[H_2W_{10}O_{32}]^{4-}$ in CH_3CN at 300 K support retention of the $W_{10}O_{32}$ frame up to two-electron reduction[26] and that the added electrons are delocalized over all ten WO_6 sites at room temperature. Thus, $[H_2W_{10}O_{32}]^{4-}$ is diamagnetic, due to both two-electrons' spin pairing in the s.o.m.o. and antiferromagnetic coupling through the W–O–W bridge (111.1—118.7° bond angles)[26] between the equatorial and capped edge-shared WO_6 octahedra. As shown in Table 4, the addition of two electrons causes an upfield shift for all equatorial W atoms, indicating increased nuclear shielding on the equatorial W atoms. The delocalization of the added electrons in the s.o.m.o. consisting of the orbital mixing among four sets of the $p\pi$–$d\pi$–$p\pi$–$d\pi$–$p\pi$ O=W–O–W=O bonding would result in π-bond weakening of the W–O bonds at the eight equatorial sites, since the s.o.m.o. should be an antibonding molecular orbital.[11] Such π-bond weakening is reflected by the upfield shift of ^{17}O resonances for both terminal W=O bonds and the linear bridging $d\pi$–$p\pi$–$d\pi$ W–O–W bonds relative to the corresponding resonances in $[W_{10}O_{32}]^{4-}$, as shown in Table 4 where the chemical shift of the terminal oxygens must be a weighted average for two oxygens at capped sites and eight oxygens at equatorial sites. On the other hand, the hopping electrons cause oscillations in magnetic fields which would allow nuclear shielding to be decreased on the n.m.r. time-scale due to a polarization effect. Such a paramagnetic effect on the

shielding, which will be dominant for the *p*- or *d*-character electrons, explains the downfield contribution to the ^{183}W chemical shift for the capped W atoms upon reduction (Table 3). The downfield contribution to the ^{183}W chemical shift by the hopping electrons has been observed for α-$[SiW_{12}O_{40}]^{6-}$ in which two added electrons are delocalized over all 12 W atoms:[27] the chemical shift (−43 p.p.m.) upon reduction of $[SiW_{12}O_{40}]^{4-}$ (at −103 p.p.m.) is downfield by +60 p.p.m. However, it is important to note that six-electron addition into the Keggin structural anion implies a different mechanism (metal–metal bonding) of the electron delocalization, probably due to a structural change in the anion. Figure 11 shows ^{183}W n.m.r. spectra of $[BW_{12}O_{40}]^{5-}$ and $[H_xBW_{12}O_{40}]^{x-11}$. The spectrum of $[H_xBW_{12}O_{40}]^{x-11}$ consists of three simple lines at 1 412.3, −109.8, and −128.3 p.p.m. with an intensity ratio of 1:1:2. Each of the lines is shifted downfield relative to a single resonance at −129.5 p.p.m. for the oxidized parent $[BW_{12}O_{40}]^{5-}$. The line at 1 412.3 p.p.m. is shifted especially strongly downfield and assigned to three W atoms in the W_3O_{13} cap where six electrons will be delocalized preferentially.[28–30] The strong downfield contribution of the line at 1 412.3 p.p.m. due to six electrons supports formation of a W–W bonded $W^{IV}{}_3O_{13}$ cluster rather than the hopping delocalization.[30]

Acknowledgements

Excimer-laser-flash photolysis (308 nm) was performed in Professor M. Kotani's laboratory at Gakushuin University. We gratefully acknowledge helpful discussions regarding measurements with Professor M. Kotani and Dr. S. Ishisaka.

References

1 T. Yamase and T. Ikawa, *Inorg. Chim. Acta*, 1979, **37**, L529; 1980, **45**, L55; T. Yamase, *ibid.*, 1981, **54**, L165; 1982, **64**, L155; 1983, **76**, L25.
2 T. Yamase, R. Sasaki, and T. Ikawa, *J. Chem. Soc., Dalton Trans.*, 1981, 628.
3 T. Yamase, N. Takabayashi, and M. Kaji, *J. Chem. Soc., Dalton Trans.*, 1984, 793.
4 T. Yamase and R. Watanabe, *J. Chem. Soc., Dalton Trans.*, 1986, 1669.
5 T. Yamase and T. Kurozumi, *J. Chem. Soc., Dalton Trans.*, 1983, 2205.
6 T. Yamase and T. Kurozumi, *Inorg. Chim. Acta*, 1984, **83**, L25.
7 R. Akid and J. R. Darwent, *J. Chem. Soc., Dalton Trans.*, 1985, 395; A. Ioannidis and E. Papaconstantinou, *Inorg. Chem.*, 1985, **24**, 439; E. N. Savinov, S. S. Saidkhanov, V. N. Parmon, and K. I. Zamaraev, *Dokl. Akad. Nauk SSSR*, 1983, **269**, 1.
8 C. L. Hill and D. A. Bouchard, *J. Am. Chem. Soc.*, 1985, **107**, 5148.
9 T. Yamase, Proceedings 1984 International Chemical Congress Pacific Basin Soc., Honolulu, Hawaii, 1984, 07553.
10 J. Muzart and J-P. Pete, *J. Chem. Soc., Chem. Commun.*, 1980, 257.
11 T. Yamase, *J. Chem. Soc., Dalton Trans.*, 1987, 1597.
12 M. Filowitz, R. K. C. Ho, W. G. Klemperer, and W. Shum, *Inorg. Chem.*, 1979, **18**, 93.
13 C. R. Deltcheff, M. Fournier, R. Frank, and R. Thouvenot, *Inorg. Chem.*, 1983, **22**, 207.
14 C. A. Parker, *Proc. R. Soc. London, Ser. A*, 1953, **220**, 104.
15 P. de Mayo, J. B. Stothers, and W. Templeton, *Can. J. Chem.*, 1961, **39**, 488.
16 S. C. Termes and M. T. Pope, *Inorg. Chem.*, 1978, **17**, 500.
17 M. A. Fedotov, L. P. Kazanskii, and V. I. Spitsyn, *Dokl. Akad. Nauk SSSR*, 1983, **272**, 1179.
18 J. S. Bradshaw, *J. Org. Chem.*, 1966, **31**, 237.
19 D. R. Arnold, P. C. Wong, A. J. Maroulis, and T. S. Cameron, *Pure Appl. Chem.*, 1980, **52**, 2609.
20 F. D. Lewis and R. J. DeVoe, *Tetrahedron*, 1982, **38**, 1069.
21 M. B. Robin and P. Day, *Adv. Inorg. Chem. Radiochem.*, 1967, **10**, 247.
22 C. Sanchez, J. Livage, J. P. Launay, M. Fournier, and Y. Jeannin, *J. Am. Chem. Soc.*, 1982, **104**, 3194.
23 B. Movaghar, L. Schweitzer, and H. Overhof, *Philos. Mag., Part B*, 1978, **37**, 683; I. G. Austin and N. F. Mott, *Adv. Phys.*, 1969, **18**, 41.
24 A. Chemseddine, C. Sanchez, J. Livage, J. P. Launay, and M. Fournier, *Inorg. Chem.*, 1984, **23**, 2609.
25 C. Sanchez, J. Livage, J. P. Launay, and M. Fournier, *J. Am. Chem. Soc.*, 1983, **105**, 6817.
26 Y. Sasaki, T. Yamase, Y. Ohashi, and Y. Sasada, *Bull. Chem. Soc. Jpn.*, in the press.
27 M. Kozik, C. F. Hammer, and L. C. W. Baker, *J. Am. Chem. Soc.*, 1968, **108**, 2748.
28 J. M. Fruchart and G. Hervé, *Ann. Chim. (Paris)*, 1971, **6**, 337.
29 M. T. Pope, in 'Mixed-Valence Compounds,' ed. D. B. Brown, D. Reidel Publishing Company, Dordrecht, 1980, p. 365.
30 J. P. Launay, *J. Inorg. Nucl. Chem.*, 1976, **38**, 807; L. P. Kazansky and J. P. Launay, *Chem. Phys. Lett.*, 1977, **51**, 244; Y. Jeannin, J. P. Launay, and M. A. Seid Sedjadi, *Inorg. Chem.*, 1980, **19**, 2933.

Received 27*th January* 1987; *Paper* 7/138